Renewable Energy 239 (2025) 122086

Contents lists available at ScienceDirect

Renewable Energy

journal homepage: www.elsevier.com/locate/renene

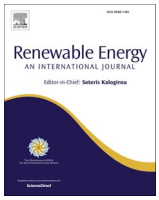

Photovoltaic soiling loss in Europe: Geographical distribution and cleaning recommendations

Álvaro Fernández Solas [a,*], Nicholas Riedel-Lyngskær [b], Natalie Hanrieder [a], Fernanda Norde Santos [a], Stefan Wilbert [a], Heine Nygard Riise [c], Jesús Polo [d], Eduardo F. Fernández [e], Florencia Almonacid [e], Diego L. Talavera [e], Leonardo Micheli [f,**]

[a] German Aerospace Center (DLR), Institute of Solar Research, Calle Doctor Carracido 44, 04005 Almería, Spain
[b] European Energy, Søborg, Denmark
[c] Department for Solar Power Systems, Institute for Energy Technology (IFE), 2007 Kjeller, Norway
[d] Solar PV Unit, Renewable Energy Division, Energy Department, CIEMAT, Avda. Complutense 40, 28040 Madrid, Spain
[e] Advances in Photovoltaic Technology (AdPVTech), CEACTEMA, University of Jaén, 23071 Jaén, Spain
[f] Department of Astronautical, Electrical and Energy Engineering (DIAEE), Sapienza University of Rome, 00184 Rome, Italy

ARTICLE INFO

Keywords:
Photovoltaics
Soiling
Mapping
Cleaning
O&M
Europe

ABSTRACT

Despite being one of the major issues that photovoltaic systems face worldwide, estimating the energy and economic magnitude of soiling of solar collectors still represents a challenge. This work presents a first European assessment of the soiling loss and of the cost-effectiveness of soiling mitigation. New soiling maps are generated through the interpolation of reanalysis data, calibrated against ground-measured losses from sensors installed across the continent. The results show that Europe experiences an average annual soiling loss of 0.9 % if rain is considered a perfect cleaning agent. However, if a cleaning effectivity by rain of 10 % is assumed, this annual loss increases up to 5.3 %. In some southern locations, soiling losses are markedly seasonal, while these are more consistent in central Europe. These losses can have repercussions on the economics of photovoltaics, increasing the levelized cost of electricity up to 4 % or 15 % depending on the cleaning effectivity of rain. The losses are also found to vary significantly in some sites from year to year, highlighting the need for continuous monitoring. The study concludes that implementing adequate soiling mitigation measures is strongly recommended in most of the regions due to the high electricity prices and the comparatively low cleaning costs.

1. Introduction

In Europe, the trajectory toward renewable energy sources, especially photovoltaic (PV) energy, mirrors global trends but with a heightened emphasis. This emphasis is underscored by the policies and initiatives implemented by the European Commission, such as the REPowerEU plan [1], which aims to elevate annual PV capacity by 600 GW by 2030, among other objectives. The report from SolarPower Europe [2] highlights that, within the European Union (EU), annual growth rates of PV capacity exceeding 40 %/year have been consistently recorded over the past four years. The growth in PV capacity has been accompanied by an increased awareness of the importance of operation and maintenance (O&M) tasks to maximize yield and performance.

The performance of PV systems can be significantly impacted by the accumulation of dirt, dust, and contaminants [3]. Airborne particles gradually accumulate on the surface of PV modules due to the interaction of various physical mechanisms, such as resuspension, deposition and cementation [4]. This phenomenon, known as soiling, reduces the intensity of the light reaching the PV cell and, therefore, the electricity output. It has been estimated to cause the loss of 4–7 % of the global PV energy yield [5]. Nonetheless, the impact of soiling on PV has been typically overlooked in Europe in comparison to other regions, like Northern Africa [6], Asia [7] and the Middle East [8], with the assumption that its effect on the final yield is negligible. However, research studies have revealed the contrary, showing that soiling can result in significant losses even in regions historically considered soiling-free due to their climatic conditions. For example, Riise et al. [9] conducted a study evaluating the impact of soiling on a PV system located at a farm in Norway, discovering that soiling losses occurred due

* Corresponding author.
** Corresponding author.
E-mail addresses: alvaro.fernandezsolas@dlr.de (Á. Fernández Solas), leonardo.micheli@uniroma1.it (L. Micheli).

https://doi.org/10.1016/j.renene.2024.122086
Received 6 May 2024; Received in revised form 8 November 2024; Accepted 2 December 2024
Available online 4 December 2024

Nomenclature

Symbols

CAPEX	Capital Expenditure [€/kW]
CoV	Coefficient of Variation [−]
CT	Cleaning Threshold of precipitation [mm/day]
d	Discount rate [%/year]
E_0	Photovoltaic energy yield without soiling [kWh/kW]
E_t	Photovoltaic energy yield with soiling [kWh/kW]
Lat	Latitude [°]
Lon	Longitude [°]
LCOE	Levelized Cost of Electricity [€/kW]
N	Lifetime, in years, of the PV system
n	Number of years since the commissioning of the PV system [−]
N_d	Constant depreciation period [20 years]
N_Y	Number of years in between two consecutive manual cleanings
NPV	Net Present Value [€/kW]
OMEX	Operation and Maintenance Expenditure [€/kW]
p	Average price of electricity [€/kWh]
$PM_{10\text{-}2.5}$	Particulate Matter concentration of particulates between 2.5 μm and 10 μm [g/m^3]
$PM_{2.5}$	Particulate Matter concentration of particulates smaller than 2.5 μm [g/m^3]
PR_{ac}	Performance Ratio after a manual cleaning event [−]
PR_{bc}	Performance Ratio before a manual cleaning event [−]
PW [DEP]	Present Worth of tax depreciation [€/kW]
PW [PV_{OM}]	Present Worth of operation and maintenance [€/kW]
r_d	Degradation rate [%/year]
r_{om}	Average annual increase rate of the OMEX [%/year]
r_p	Average annual increase rate of the electricity price [%/year]
S_L	Soiling loss [%]
$\overline{S_L}$	Arithmetic mean soiling loss [%]
$\overline{S_{L\_IW}}$	Irradiance-weighted average soiling loss [%]
$\overline{S_{L\_E}}$	Energy-weighted average soiling loss [%]
S_m	Cumulative soiling loss accumulated over a month [%]
S_{m_sum}	Cumulative soiling loss accumulated over a year [%]
SVI	Soiling Variability Index [−]
SR	Soiling Ratio [%]
T	Income tax rate [%/year]
t	Accumulation period [s]
$v_{10\text{-}2.5}$	Settling velocity of particulates between 2.5 μm and 10 μm [m/s]
$v_{2.5}$	Settling velocity of particulates smaller than 2.5 μm [m/s]
w	Total accumulated mass [g/m^2]
WACC	Weighted Average Cost of Capital [−]
θ	Tilt angle of the PV modules [°]

Abbreviations

ADS	Atmosphere Data Store
CAMS	Copernicus Atmosphere Monitoring Service
EAC4	ECMWF Atmospheric Composition Reanalysis 4
ECMWF	European Centre for Medium-Range Weather Forecasts
EU	European Union
IRENA	International Renewable Energy Agency
LED	Light Emitting Diode
O&M	Operation and Maintenance
PV	Photovoltaics
PVGIS	Photovoltaic Geographical Information System
USA	United States of America

to agricultural activities in the vicinity of the PV site. Appels et al. [10] found that high pollen concentrations can cause a 3–4 % energy yield loss in Belgium. Furthermore, Saharan dust intrusions have been reported in both southern and northern European countries [11,12], and can accelerate the accumulation of soiling, leading to significant losses [13].

In light of these observations, acquiring precise knowledge of the magnitude of soiling losses becomes essential. This information can be obtained through either on-site monitoring, which typically consists of using either specialized sensors [14–18], or modeling approaches [19–22]. The use of models allows estimating the losses without the need of specific hardware and of data collection campaigns, as soiling can be estimated from widely available environmental datasets.

Because of their potentially easier implementation, several modelling approaches have been proposed through the years. The study of Kimber et al. [23] pioneered the development of PV soiling models. Their model calculates the PV energy losses due to soiling by assuming a daily soiling rate, which indicates how much energy loss increases per day. It also includes a cleaning threshold (CT) for rainfall, which determines whether a rain event is sufficient to completely remove soiling from the surface of the modules, and a grace period, which represents the time the PV system remains clean after rainfall. While widely employed, the so-called Kimber model still requires the knowledge of the power derate caused by soiling. This information, however, might not be available, especially when soiling at a new site is assessed. For this reason, environmental-data-based soiling models were introduced, allowing to estimate also the power derate due to soiling from environmental parameters. The seeds of such models were those studies that identified the correlations between individual environmental parameters and specific soiling mechanisms [24–27]. For instance, Jiang et al. [24] conducted an indoor experimental investigation to correlate airborne dust deposition and the performance loss of PV modules. They found a linear relationship between the dust deposition density and the reduction in PV output efficiency, encountering a maximum drop of 26 % with 22 g/m^2 of dust density. Similarly, through an outdoor experiment, also Boyle et al. [25] found a linear correlation between the mass of dust accumulated on a glass and the loss in transmittance. Bergin et al. [26] studied the influence of both ambient and deposited particulate matter (PM) on the reduction of the available energy for solar power production. They also estimated the relative contribution of the different PM components to the decrease in PV module transmittance. Javed et al. [27] used an Artificial Neural Network approach to model the relationships between environmental variables, such as PM concentration, wind speed and direction, temperature and relative humidity, with the performance loss due to soiling. They found that both wind speed and relative humidity were the two environmental parameters that most affect the airborne dust accumulation on the surface on PV modules, and thus impact their energy output.

Following those studies, different multi-variable empirical models were developed to reproduce both the removal and deposition mechanisms, and therefore generating a soiling loss profile [19,20,28]. Coello et al. [19] presented a model that uses PM concentrations, the tilt of the PV modules and rain data to simulate the temporal evolution of soiling losses at a site. The model first calculates the accumulated mass on the surface of the modules, and then it estimates the transmission losses using an empirical equation. It assumes that any day with an average daily precipitation intensity higher than a certain threshold totally removes the accumulated mass. The model was initially tested using measured soiling data from seven locations across the southwestern United States. You et al. [29] presented an approach that estimates the dust deposition density as a function of the deposition velocity, the PM concentrations and the length of dry spells. Then, it models the loss in

efficiency of PV by considering the linear rate of 0.0139 %/g suggested by Jiang et al. [24]. They applied the model to various cities worldwide without further validation. Toth et al. [28] also proposed a model based on PM concentration and rainfall to predict daily soiling losses. However, conversely to Coello's one, this considers that rainfalls can only remove coarse particulates (particulates with a diameter higher than 2.5 μm), while fine ones are only washed off from the surface of PV modules after artificial cleanings. The model presents two parameters that requires site-specific calibration. Originally, the authors fitted these parameters using measured soiling data from an urban-industrial location in Colorado, United States.

In recent years, several studies have been published in an attempt to compare, customize and assess the performance of the previously presented models in different locations. Sharma et al. [30] compared three environmental-based soiling models with field soiling measurements in a semi-arid location in India. They found that Coello's model overestimated the losses, while Toth and You models slightly underestimate them. Bessa et al. [31] conducted a benchmarking assessment of four different environmental-based soiling models in Jaén, southern Spain. They used satellite-derived data as inputs and tuned the model coefficients to align with the local conditions of the site. In addition, they conducted a sensitivity analysis to evaluate how different values of rain-cleaning threshold impact the soiling profile. They found that Coello and You models were the ones that performed the best, returning the lowest errors when compared against actual soiling measurements, for the selected location. Polo et al. [22] modeled the soiling losses of a PV system located in an area with nearby forest in Madrid, Spain using Coello's model with dynamic deposition velocities and a cleaning threshold of 4 mm/day. They validated the simulations with measured soiling data and concluded that better agreements were found during the summer season, while the larger discrepancies occurred during periods with frequent rainfalls, thus highlighting the need for an appropriate selection of the cleaning threshold and casting doubt on the complete rain's cleaning effectivity. Lara-Fanego et al. [32] presented a study that showed different possible parametrizations and adaptations of Coello's model parameters to the realistic conditions of PV systems located in regions with different climates. Their work aimed to improve Coello's model accuracy and global reliability.

More recently and based on previous approaches that rely on environmental parameters, new PV soiling models have been generated, such as the machine learning models proposed by Lopez-Lorente et al. [33] and tested in a location with a dry climate in Cyprus, the numerical model proposed by Redondo et al. [34], which was validated with specific soiling data from five different large PV systems in Spain, or the Artificial Neural Network method developed by Laarabi et al. [35] using data collected in Morocco.

However, as introduced earlier, modeling soiling patterns has traditionally relied on theoretical frameworks and data from a limited number of locations [36]. The present study leverages a novel empirical dataset, exploring the soiling dynamics across different spatial and temporal scales. The empirical data used in this study comprises an extensive set of field soiling measurements collected through specialized sensors deployed across diverse European locations. These allow the recalibration of the soiling deposition and removal model, thus enhancing its accuracy, as its default parameters were initially derived from observations at only seven sites across the USA [19]. Additionally, this study incorporates historical reanalysis-generated meteorological and environmental parameters for the past 15-year period. This way, the temporal variability of soiling can be assessed at different scales (seasonally and yearly) across a region of unprecedented extension.

In addition to the energy loss, the economic assessment of the soiling impact holds as well vital importance in order to make informed decisions related to soiling mitigation activities. An accurate understanding of the profitability and the cost-effectiveness of cleaning activities can determine whether it makes sense to remove the soiling from the PV modules at a certain moment. In this light, accurate and high-resolution maps of soiling can efficiently inform on the optimized cleaning schedules to enhance energy production. For this reason, this work also presents assessments of the economics of the soiling loss and soiling mitigation. This way, the economic viability of cleaning can be evaluated, in light of the current costs and of the expected benefits for the various locations considered in this study.

Overall, the key objectives of the present research are twofold: first, to map both energy and economic losses in PV systems due to soiling patterns, and second, to share with the community a modified version of a soiling model that allows to customize the cleaning effectiveness of rain, which could be reapplied in additional studies. The maps and the models not only offer insights into the spatial distribution of soiling, but also provide a valuable resource for stakeholders involved in decision-making processes related to maintenance planning, resource optimization, and environmental impact assessments. However, it is important to note that the used model provides information at high granularity, offering a regional perspective on the expected soiling losses, but does not account for the local conditions and therefore may not accurately reproduce the specific conditions of a site.

The paper is organized as follows. The methodological steps are described in Section 2. These include the procedures employed to assess the soiling pattern and to recalibrate the soiling model (2.1), the adaptation of the employed model to consider the rain's cleaning effectivity (2.2), as well as the methods used to conduct the economic analysis (2.3). The results are then presented in Section 3. These are comprised of a description of the novel recalibrated model inputs (3.1), an assessment of the energy loss magnitude and variability (3.2), a cost/benefit analysis of soiling loss mitigation through cleanings (3.3), and a detailed discussion of the impact of rain's cleaning effectivity on the results (3.4).

2. Methodology

2.1. Soiling metrics and model

The magnitude of the soiling losses can be estimated through models based on environmental parameters [36]. These do not only allow monitoring the losses without a soiling sensor, but make it possible to estimate soiling in any location where environmental data are available. Of the various approaches proposed in the literature, the present work makes use of the model developed by Coello and Boyle [19]. In this approach, the soiling loss is modeled to build up from the deposition of particulate matter (PM) on the surface of PV modules. The model assumes that the deposition rates can be estimated from the PM concentration, and that daily rainfall exceeding a certain threshold [mm/day] can completely wash off soiling. The PM concentration is typically quantified using two indicators, PM_{10} and $PM_{2.5}$, which represent the masses of suspended particulates per m^3 of air with diameters up to 10 μm and 2.5 μm, respectively.

Equation (1) for calculating the magnitude of soiling loss (S_L) [−] on a d-day is given by:

$$S_L(d) = 0.3437 \bullet \mathrm{erf}\left(0.17 \bullet w(d)^{0.8473}\right) \quad (1)$$

where w [g/m^2] represents the total accumulated mass of particulates on the PV surface since the last cleaning event, which can be either a rainfall higher than a threshold or an artificial cleaning. This accumulated mass on a day d is calculated using equation (2):

$$w(d) = \sum_{d_0}^{d} \left[\left(v_{10-2.5} \bullet PM_{10-2.5}\right) + \left(v_{2.5} \bullet PM_{2.5}\right)\right] \bullet t \bullet \cos\theta \quad (2)$$

where $PM_{10\text{-}2.5}$ and $PM_{2.5}$ represents the mass of particulates per m^3 of air [g/m^3] with diameters between 2.5 μm and 10 μm and lower than 2.5 μm, respectively; $v_{10\text{-}2.5}$ and $v_{2.5}$ are the deposition velocities of $PM_{10\text{-}2.5}$ and $PM_{2.5}$ in m/s, t denotes the accumulation period expressed in seconds, and θ [°] is the tilt angle of the PV modules. The

accumulation period starts on the d_0-day, the first day after the last cleaning event.

In this work, the model was fed with daily EAC4 global reanalysis particulate matter data and ERA5 precipitation data for the 2005 to 2019 period downloaded from the Copernicus Atmosphere Monitoring Service (CAMS) Atmosphere Data Store (ADS) [37]. In addition, a novel dataset of field soiling measurements gathered from various sites across Europe (see Table S 1) was employed to recalibrate the model. This recalibration was needed to incorporate in the model additional factors influencing soiling losses, such as changes in land use or human activities. The necessity for fine-tuning environmental-data-based soiling models was previously highlighted in Ref. [38], where the authors demonstrated that soiling estimations produced with the same models can generate dissimilar results when fed with data from different sources.

As aforementioned, the recalibration was conducted by utilizing actual soiling data measured at nine different sites across Europe, whose distribution and measurements are shown in Fig. 1. That figure also includes a special case study from Switzerland, presented in the IEA PVPS Task 13 report on soiling [36]. At this site, located next to a railway station, significant soiling losses were observed despite the regular precipitations. Soiling losses were not directly measured, but were instead inferred by comparing the performance ratio of the PV system before and after manual cleanings. The purpose of including this site is to demonstrate one of the limitations of the original version of the soiling model used and to allow the estimation of the soiling losses for the case of incomplete cleaning by rain. A more detailed explanation is provided in Section 2.2.

The measurements of the average annual soiling losses, ranging from 0.35 to 1.84 %, were obtained through specialized equipment, including an Atonometrics® soiling station [39] and DustIQ optical soiling sensors from Kipp&Zonen [40], except for the Swiss site, which was not used for recalibrating the original parameters of the model, but for adjusting a novel one (see Section 2.2).

Soiling stations often consist of two identical PV devices: one regularly cleaned and the other left to accumulate natural soiling. These stations calculate soiling loss by directly comparing the electrical output of both devices. On the other hand, DustIQ sensors estimate soiling loss through changes in scattering measurements. A modulated photodiode measures the amount of light emitted from an LED and reflected from the dust particulates deposited on the surface of a PV glass coupon. For sites equipped with DustIQ sensors, the raw data were corrected using calibration coefficients provided by the sensor operators. These coefficients were obtained to account for the typical dust types present at the PV site. An Atonometrics® soiling station was only used in one of the Spanish sites. It was periodically calibrated during the experimental campaign to ensure accurate soiling measurements, thus avoiding a potential impact of mismatch between the two PV devices on the results. The reference device was automatically cleaned daily using a pressurized water spray. It is important to note that, despite the use of different soiling monitoring equipment, the final daily soiling loss values remained unaffected, as appropriate raw data pre-processing methodologies were applied to each dataset. Further details about the experimental sites are displayed in Table S 1, in the Supplemental Material. The results of the recalibration process are presented and discussed in Section 3.1. The soiling loss data feature a wide range of tilt angles and one single-axis-tracking system. These tilt angles have been considered in the calibration procedure as lower tilt angles are generally associated with higher soiling losses [10]. Evaluating the specific impact of tilt angle on soiling accumulation is beyond the scope of this paper, as the employed soiling model accounts for the effect of angle. In this study, the soiling loss at each location is estimated for the optimal tilt and azimuth angles, calculated by PVGIS [41].

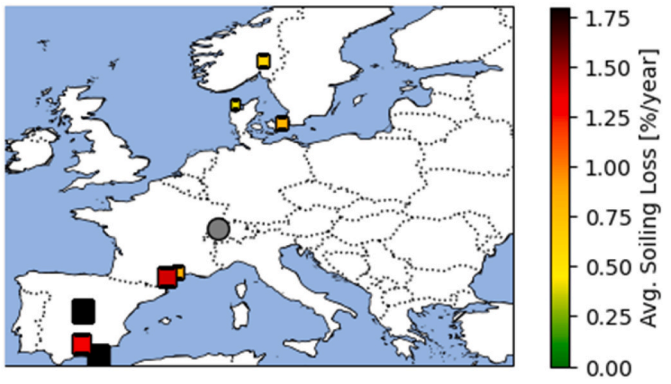

Fig. 1. Locations of the experimental sites. The color and the size of the squared markers are indicative of the magnitude of the measured soiling loss. The Swiss site is represented with a circular marker as the soiling losses were not directly measured there, but only derived from PV performance data before and after the manual cleaning.

The annual average loss experienced by a site is typically expressed as the arithmetic mean of the daily values (S_L), calculated by averaging all the measurements recorded by the sensors within 1 h of the solar noon as indicated in equation (3):

$$\overline{S_L} = \frac{\sum_{d=1}^{T} S_L(d)}{T} \tag{3}$$

where $S_L(d)$ is the soiling loss [−] on a day d and T represents the total number of days in the analyzed period.

To ensure the reliability of the measurements, data points affected by precipitation, dew, or frost were filtered out prior to calculation. This is considered to be acceptable as such conditions often occur for low irradiances. However, it must be acknowledged that the actual impact of soiling varies depending on the weather patterns. Indeed, if soiling occurs in the season of highest solar irradiance, its impact can be expected to be higher than that estimated from the arithmetic mean. For this reason, the soiling loss calculated as arithmetic mean of the daily data ($\overline{S_L}$) is here compared with the irradiance-weighted mean ($\overline{S_{L\_IW}}$) [−], which is calculated using equation (4):

$$\overline{S_{L\_IW}} = \frac{\sum_{d=1}^{T} S_L(d) \bullet POA(d)}{\sum_{d=1}^{T} POA(d)} \tag{4}$$

where T is the total number of days in the analyzed period, and POA(d) is the daily plane-of-array irradiation on a given day d.

In addition, one should consider that additional factors, such as the cell temperature, influence the output of the PV cell. Therefore, in order to evaluate the accuracy of the arithmetic and irradiance-weighted mean for soiling loss estimation, these are also compared with the soiling-induced energy loss (S_{L_E}), calculated through equation (5):

$$\overline{S_{L\_E}} = 1 - \frac{\sum_{d=1}^{T} (1 - S_L(d)) \bullet E_0(d)}{\sum_{d=1}^{T} E_0(d)} \tag{5}$$

where E_0 [kWh/day] is the daily energy yield on day d, excluding any loss due to soiling. This was downloaded for each location for the 2004 to 2019 period from PVGIS [42]. Optimal tilt and azimuth angles were assumed, calculated by PVGIS [41]. Fixed losses of 12 % were set, removing the 2 % typically attributed to soiling from the 14 % default value [43]. The 15-year data have been repeated twice to generate a 30-year long time series. This is indeed the standard reference period for climate assessment studies as it allows capturing both seasonal and long-term trends. However, it is acknowledged that this might not be

able to capture future variations induced by climate change. Attempting to model these would have introduced additional uncertainty in the results.

In addition to the average yearly loss, additional characteristics of soiling have been assessed in this work, but, for the sake of simplicity, only for the original version of the model that considers full cleaning by rain above a certain threshold. Indeed, the soiling losses are not uniform over the year [44], but tend to concentrate in seasons with least frequent and intense rainfall and/or higher particulate matter concentrations. Additional factors can contribute to the seasonal variation of soiling, including, for example, human activities. In this work, the seasonal variation of soiling has been quantified through the "Soiling Variability Index" (SVI), an unitless index originally proposed in Ref. [45]. This metric, adapted from the seasonality index [46], a commonly employed index to evaluate the monthly accumulated rainfall values, is calculated as sum of the absolute deviations of the losses accumulated on a month from the monthly average, divided by the total yearly loss as shown in equation (6):

$$SVI(site) = \frac{\sum_{m=1}^{12} \left| S_m(m) - \frac{S_{m\_sum}}{12} \right|}{S_{m\_sum}} \quad (6)$$

where S_{m_sum} is the sum of the soiling losses (S_m) accumulated in each month m over a year. S_{m_sum} and S_m are calculated by using equations (7) and (8), with n_d representing the number of days in a month:

$$S_{m\_sum} = \sum_{m=1}^{12} S_m(m) \quad (7)$$

$$S_m(m) = \sum_{s=1}^{n_d} S_L(d) \quad (8)$$

SVI varies between zero (no variability: same soiling in each month) to 1.83 (maximum variability: all losses occur in just one month).

In addition to seasonal patterns, soiling can exhibit also fluctuations over the years [44,47], a phenomenon that has been defined as interannual-variability. This variability is induced by multiple factors, which include climatic conditions, geographical location, land use, and human activities. In this work, the inter-annual variability of soiling has been quantified through the coefficient of variation (CoV), an unitless metric calculated as ratio of the standard deviation to the mean of the yearly averages as shown in equation (9):

$$CoV(site) = \frac{\sigma_{S_{L_y}}}{\overline{S_{L_y}}} = \frac{\sqrt{\sum \left(S_L(y) - \overline{S_{L_y}}\right)^2 / N}}{\sum S_L(y)/N} \quad (9)$$

where $\overline{S_{L_y}}$ [%] is the mean soiling loss over the investigated period, $\sigma_{S_{L_y}}$ [%] is the standard deviation, $S_L(y)$ is the mean soiling loss in the year y, and N is the number of investigated years.

2.2. Adapted version of the soiling model

The model presented above assumes a perfect cleaning after each rain day of intensity above the threshold. However, there are evidences that refute this hypothesis of rain being a perfect cleaning agent. For example, Javed et al. [48] found that the cleaning effectiveness varies depending on the soiling loss and on the rain intensity. Norde Santos et al. [49] found that in most cases rain did not completely remove the soiling accumulated on systems deployed in various West African locations. Additionally, other types of soiling such as pollen, bird droppings and industrial pollutants are likely to stay adhered to the surface of PV modules until a proper artificial cleaning is conducted. Furthermore, in some cases, rain can also have a negative impact, e.g. by promoting wet deposition of aerosols particulates present in the atmosphere onto the modules [5].

For this reason, in the last part of this work, the soiling model is modified to consider the limited cleaning effectiveness of rainfall. The novel model is tested using data from a case study of a system located in a rainy location (>1000 mm year^{-1}) with a uniform precipitation distribution in Switzerland, where losses of up to 10 % due to soiling were identified after artificially cleaning the system (see Fig. 2) [36]. The losses due to soiling are derived by comparing the performance ratio (PR) of the system, which represents the ratio of the actual and theoretical power outputs, after and before a manual cleaning by means of equation (10).

$$S_L[\%] = \frac{PR_{ac} - PR_{bc}}{PR_{ac}} \bullet 100\% \quad (10)$$

where PR_{ac} and PR_{bc} represent the performance ratio of the PV system after and before of a manual cleaning, respectively. The soiling loss reached one year after the last manual cleaning ($S_{L\_avg_a}$) is calculated according to equation (11):

$$S_{L\_avg_y}\ [\%] = \frac{S_L\ [\%]}{N_Y} \quad (11)$$

where N_Y is the number of years in between two consecutive manual cleanings.

To partially address this completeness of cleaning by rainfalls, a novel parameter, called "Cleaning Factor" has been introduced in the soiling model. It is calculated through equation (12):

$$Cleaning\ Factor = 1 - \frac{accumulated\ mass\ after\ rainfall > CT}{total\ accumulated\ mass} \quad (12)$$

This dimensionless parameter represents the fraction of accumulated mass that can be washed off by a rain event with an intensity exceeding the CT. It can help improve the modeling of soiling accumulation and removal processes, particularly in locations where the soiling types are more resistant to the cleaning effect of rain. The recalibration of the model after incorporating this novel parameter is shown in section 3.1.1.

2.3. Economic analysis

The economic analysis presented in this work evaluates two of the most common economic metrics in PV studies. These were calculated by using the methodology and the input parameters described in Ref. [50].

The first economic metric is the levelized cost of electricity (LCOE), which expresses the cost of producing a kWh of electricity over the system lifetime. It is expressed in €/kWh and should be as low as possible. It was calculated as in Ref. [51] by using equation (13):

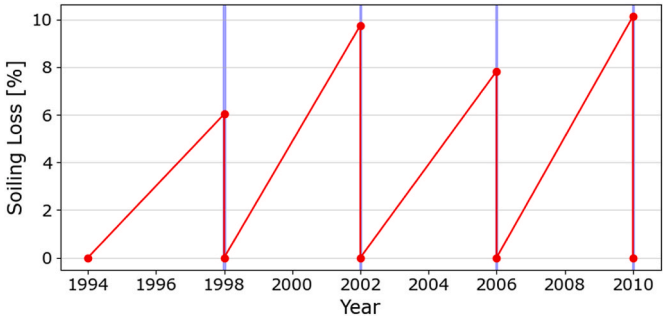

Fig. 2. Soiling losses in a PV installation located close to a railway station in a rainy region in Switzerland. Significant soiling losses can be appreciated between 1994 and 2010 by comparing measurements conducted before and after artificial cleanings. The vertical blue bars represent the years when artificial cleanings were conducted. Data extracted from Figure 28 in Ref. [36].

$$LCOE = \frac{CAPEX + PW[PV_{OM}(N)] - PW[DEP(N_d)]}{E_t \bullet \sum_{n=1}^{N} \frac{(1-r_d)^n}{(1+d)^n}} \quad (13)$$

where $CAPEX$, $PW[PV_{OM}(N)]$, $PW[DEP(N_d)]$, E_t, r_d, N, and d are, respectively, the capital expenditure in €/kW, the present worth of operation and maintenance in €/kW, the present worth of tax depreciation in €/kW, the annual energy yield in kWh/kW, the annual system degradation rate (set to 0.75 %/year according to Ref. [52]), the lifetime of the system (equal to 30 years), and the discount rate [%/year], set equal to the organization's weighted average cost of capital (*WACC*) [45]. Tax depreciation is assumed to last for a period N_d of 20 years [53]. The country-specific CAPEX values were taken from the 2023 IRENA report on renewable energy costs, and are reported in Supplemental Material (Table S 2) [54].

The lifetime operation and maintenance costs were calculated using equation (14):

$$PW[PV_{OM}(N)] = \sum_{n=1}^{N} \frac{OMEX \bullet (1-T) \bullet (1+r_{om})^n}{(1+d)^n} \quad (14)$$

where $OMEX$ is the annual operation and maintenance expenditure in €/kW (also set in accordance with [54]), r_{om} [%/year] is the rate at which it annually increases and T [%/year] is the income tax rate. The values of the last two parameters for each country were set as in Ref. [50].

The present worth of tax depreciation term was calculated through equation (15), assuming a 5 % linear and constant depreciation for 20 years (N_d), as:

$$PW[DEP(N_d)] = \sum_{n=1}^{N_d} \frac{5\% \bullet \text{CAPEX}}{(1+d)^n} \bullet T \quad (15)$$

While providing information on the costs of energy generation, the LCOE does not assess the profitability of PV. This can be done through the net present value (NPV) [€/kW], which expresses the difference between the present values of the cash flows (in and out) generated throughout the lifetime of the project. A positive NPV is a necessary condition for a profitable investment. The NPV can be calculated as in Ref. [51] using equation (16):

$$NPV = -CAPEX + p \bullet E_t \bullet \sum_{n=1}^{N} \frac{(1-r_d)^n}{(1+d)^n} \bullet (1+r_p)^n \bullet (1-T) - PW[PV_{OM}(N)] + PW[DEP(N_d)] \quad (16)$$

where p [€/kWh] is the average price of electricity and r_p [%/year] is its average annual increase rate. The average electricity price for each country was set equal to the mean of the daily values in the 2010 to 2021 period, sourced from the websites of the country-s market operators [55–72]. Additionally, the yearly increase in electricity price (r_p) was set equal to the average of the 2010 to 2021 inflation [50].

3. Results & discussion

3.1. Soiling model recalibration

As described earlier, the soiling model has been recalibrated using an extensive dataset of field soiling measurements from nine European locations (Fig. 1). The measurements taken by the soiling sensors were pre-processed and filtered according to the instructions provided by the manufacturers. Fig. 3 shows the procedure followed to calculate the daily average soiling loss from the raw measurements of the sensors. This eliminated the influence of factors such as incidence angle, dew, or rain, which could affect soiling measurements.

The recalibration involved identifying the optimal pair of values for deposition velocity and CT values that minimized the average modeling error across locations with measured data. To streamline the process, a uniform deposition velocity value for both $PM_{10\text{-}2.5}$ and $PM_{2.5}$ was considered. Regarding the CT, as mentioned earlier, previous studies have demonstrated that selecting a single daily accumulation value does not fit all cleaning events in PV systems [48,73]. This is because the effectiveness of cleaning depends on various factors, including the magnitude of soiling losses and the physical and chemical properties of the accumulated dust.

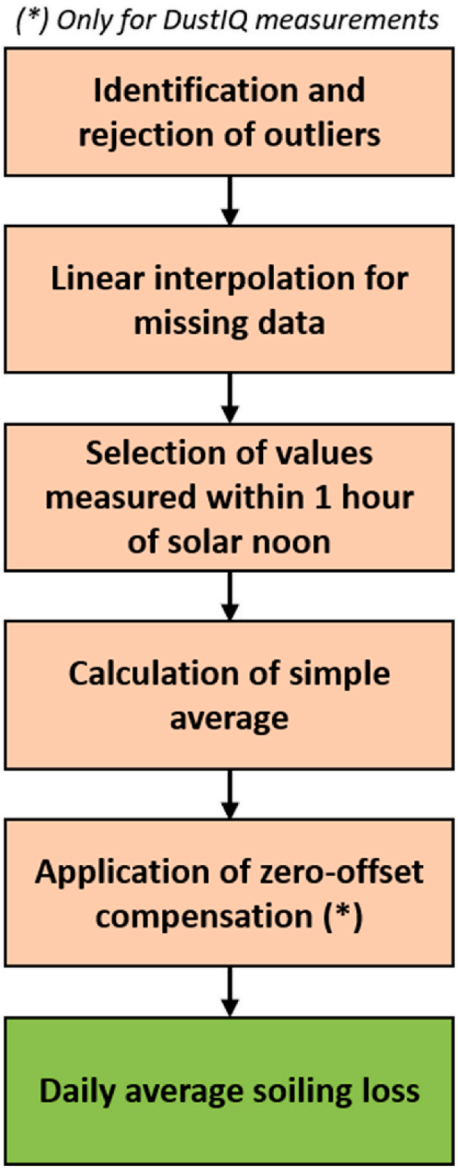

Fig. 3. Flowchart of the approach followed to calculate the daily average soiling loss from the sensors' raw measurements.

The methodology of the model recalibration comprised three stages. In the initial stage, the soiling profile of each site was modeled, considering various CTs: 0.2, 1.0, 3.0, and 5.0 mm/day. Through visual inspection and comparison against the measured data, it was observed that using a CT < 3 mm/day led to the detection of false cleaning events at some sites. Consequently, the two smallest CTs were excluded from the subsequent stages.

In the second stage, for CTs of 3.0 and 5.0 mm/day, the deposition velocity was systematically varied from 0.1 cm/s to 5.0 cm/s with a step of 0.1 cm/s. For each site and combination of CT and deposition velocity, the average modeled soiling ratio (1 – soiling loss) was calculated. The soiling ratio represents the ratio of the power output of a soiled

module to that of a clean one under the same conditions. A ratio of 1 means that there is no soiling. On the other hand, the soiling loss indicates the fraction of power lost due to soiling, thus, a value of 1 indicates that all the power is lost because of soiling.

The final stage involved comparing the modeled and measured average annual soiling loss for the set of sites. Linear regression was employed to fit the values, revealing that the combination of a CT of 5.0 mm/day and a deposition velocity of 0.9 cm/s produced the most favorable results, with a slope equal to 1.00 and an R^2 of 0.49, as it can be seen in Fig. 4. Additionally, the differences in the average values of soiling ratio between the measured and modeled profiles ranged from −0.78 % to +0.84 %. The relatively high final CT value obtained compared to the model's default value (1 mm/day) suggests that the model performs more effectively in regions with consistently low soiling losses throughout the year, such as Scandinavian countries. Conversely, in areas where soiling is predominantly seasonal, with the majority of losses occurring during summer months, days with precipitation below the CT can partially clean the modules. This is a factor not accounted for by the model, potentially leading to overestimations of losses. On the other hand, this first version of the model used in this work, which also considers full cleaning above the CT, might lead to underestimations of the losses in some cases. These disparities highlight the challenges in accurately estimating the soiling losses in PV systems, as local factors, such as the ground properties and the utilized measurement techniques of distinct parameters, can affect the reliability of the models. This emphasizes a further challenge: models developed and validated for specific climates may not be directly transferable to regions with different climatic conditions, or could, at least, result in greater uncertainties. Developing region-specific approaches for soiling modeling could potentially enhance their reliability and applicability across diverse climatic regions. All the aforementioned limitations also underscore the importance of both, a wide network of soiling monitors and the need for continuous validation of soiling models to increase their accuracy.

In addition, it is worth noting that the use of reanalysis data introduces some intrinsic uncertainties, that can lead to the deviations between modeled and actual data shown in Fig. 4. Datasets such as those used in this work offer a broad spatial and temporal coverage, but may not fully capture localized phenomena such as microclimates or site-specific soiling dynamics. These limitations can affect the accuracy of both input parameters (e.g., precipitation and particulate matters) and thus output predictions, especially in regions with highly variable environmental conditions. While reanalysis data are invaluable for large-scale studies, integrating them with site-specific measurements could significantly improve accuracy. This integration becomes particularly important when such models are used for real-time monitoring rather than historical soiling assessment. The latter, which is the main aim of this work, can rely on historical data to generate typical soiling profiles for any location. The former, however, requires access to real-time data and, where available, short-term forecasts to produce high-accuracy, real-time soiling estimates.

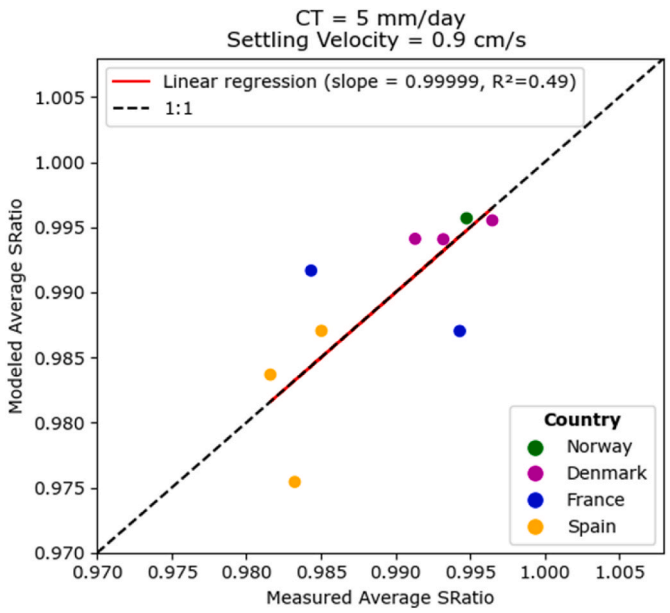

Fig. 4. Recalibration result of the evaluated soiling model with optimized parameter values for cleaning threshold (5.0 mm/day) and settling velocity (0.9 cm/s). The markers represent the average measured and modeled soiling ratio (SRatio) values at the distinct locations. The red line represents the linear fit calculated using the function "linregress" of the "SciPy" Python library [74].

3.1.1. *Modified version of the model: calibration of cleaning factor using a case study from Switzerland*

As explained in Section 2.1, the first version of the model employed to estimate the magnitude of the soiling losses assumes that rainfall events exceeding a certain threshold completely remove all the accumulated particulates, thus restoring the soiling loss to 0 %. However, as described earlier, different field studies have reported that rain cannot completely wash off soiling. For this reason, in this section, the soiling model is modified to limit the cleaning effectiveness of rain events and the novel cleaning factor parameter is calibrated by using the data reported for a system in Switzerland, which experienced, despite the consistent rainfalls, losses of up to 10 % due to soiling as shown in Fig. 2 [36]. At that site, which, on average, experiences more than 100 days per year with daily precipitations higher than the CT of 5 mm/day, assuming rain to be a perfect cleaning agent can lead to a clear underestimation of the soiling losses – the original version of the model, fed with the parameters obtained after the recalibration displayed in Fig. 4, returns an average annual soiling loss of 0.47 %, which is over five times lower than the actual extracted value of 2.53 %. This finding aligns with previous studies mentioning rain's limited ability to fully remove dirt from the surface of PV modules, thus highlighting the importance of assessing the completeness of cleaning by rain in soiling modeling.

To show the impact of accounting for the completeness of cleaning by rain in the model, the Cleaning Factor was calibrated to match with the extracted annual average soiling loss increase at the Swiss location of 2.53 % between 2006 and 2010. A Cleaning Factor of 0.1 returned the best fit, while maintaining the same combination of CT (5 mm/day) and deposition velocity (0.9 cm/s) as previously determined (see Fig. 4). This value implies that a day with a precipitation exceeding the CT only removes 10 % of the accumulated mass from the surface of the PV modules, leaving 90 % still present after the rainfall. Although this scenario may not reflect the conditions at many sites, it can be feasible in locations like the one evaluated in this paper, where train brake dust with strong adhesion properties might be a main contributor to the soiling losses. In such a case, rain events might only remove a small portion of the accumulated mass. Consequently, important long-term soiling losses can occur if periodical manual cleanings are not conducted.

Fig. 5 shows the modeled soiling profile for that location using the abovementioned parameters. Only the first year of operation is displayed without considering any manual cleanings. However, as already mentioned, if no specific cleanings are conducted, the magnitude of the soiling losses will exponentially grow in following years, therefore, leading to long-term soiling accumulation. This work also intends to inform the PV community about the importance of permanently assessing the soiling losses to avoid this negative scenario, which can notably reduce the performance of PV installations.

The modified version of the model is also used to evaluate both the soiling magnitude and the economic impact of soiling and cleanings in Europe by following the methodology detailed in Section 2.

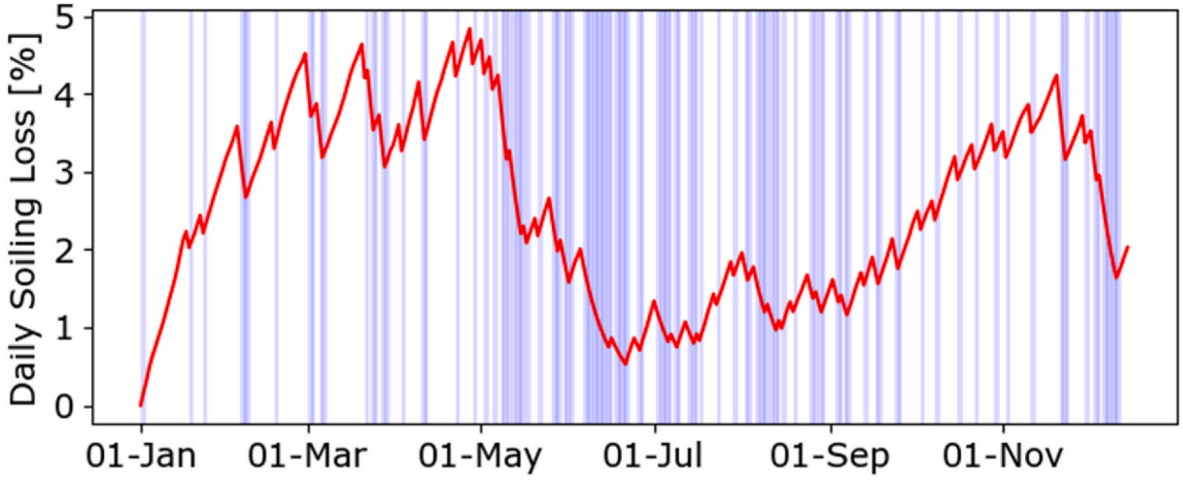

Fig. 5. Simulated annual soiling profile for the Swish location (latitude: 47.14°N, longitude: 7.25°E) using the modified version of the model with the following inputs: deposition velocity of 0.9 cm/s, cleaning threshold of 5 mm/day and cleaning factor of 0.1. The vertical blue bars represent the dates with a precipitation higher than the threshold.

3.2. Soiling: magnitude and variability

The distributions of soiling losses in the various European countries considering the original model and the modified model are shown in Figs. 6 and 7, respectively, also plotted in the maps reported in the Supplemental Material (Fig. S 1). The distributions are calculated from the average soiling loss modeled on each point of the grid. Specifically, the red bars show the arithmetic mean ($\overline{S_L}$), the blue bars show the irradiance-weighted mean ($\overline{S_{L\_IW}}$) and the green bars show the energy-weighted loss ($\overline{S_{L\_E}}$). Overall, one can see that the countries in the investigated region experience an average modeled annual soiling loss (red bars) of 0.9 ± 0.4 % (original model) and 5.3 ± 2.0 % (modified model), but the losses are not uniformly distributed. Indeed, peaks as high as 3.3 % (original model) and higher than 10.0 % (modified model) are registered in the southernmost European countries. Portugal, Türkiye, Spain, Italy, and Greece are the countries with the largest average losses, pushed by the drier climates, especially in summer. In particular, the peak losses (>12.0 % if the modified model is used) are found in selected locations of Spain and Greece. Conversely, the northern countries (Sweden, Norway, Ireland) and the alpine countries (Switzerland) show the minimum losses, with median values below 0.5 % (original model) or below 3.0 % (modified model). All of these obtained values cast doubt on the typical soiling loss assumptions commonly utilized by PV modelers or on the assumed cleaning schedules. Soiling loss assumptions in PV modelling usually range between 1.0 and 3.5 % [75]. In Nordic countries and in alpine regions, such assumptions would result in an overestimation of the losses, consequently leading to an underestimation of the final yield. Conversely, in certain locations across southern Europe, these assumptions may lead to underestimations of annual soiling losses.

Fig. 6 shows that, on average, the arithmetic mean underestimates the soiling-induced energy losses ($\overline{S_{L\_E}}$) by 16.3 ± 5.5 $\%_{rel}$. This means that this approach can lead to a severe underassessment of the impact of soiling, which can also have economic repercussions if the costs/benefits of soiling mitigation are miscalculated. Indeed, in Greece and Türkiye the annual energy loss due to soiling reaches peaks higher than 3.5 %, which are up to 1 % higher than the losses estimated through the arithmetic mean ($\overline{S_L}$). The reason behind the arithmetic mean underestimation is due to the typical soiling profile in Europe (i.e., the seasonal pattern of soiling). Losses are indeed higher in summer, where aridity and less frequent precipitations boost soiling deposition and limit removal. At the same time, irradiation is also higher in summer. This means that the larger soiling losses in summer obtain a higher weighting factor than the soiling losses in winter because of the greater irradiance that could be converted by the modules. Therefore, the energy weighted soiling losses are higher than the arithmetic average of the soiling losses in such cases.

Using the irradiance weighted mean allows reducing the miscalculation, leading to a slight overestimation of 2.4 ± 1.5 $\%_{rel}$ (blue bars in Fig. 6). Similar trends can be seen also for the modified model, in Fig. 7. This overestimation is possibly due to the effect of the temperature, which is typically higher in summer and which negatively affects the PV performance, partly counteracting the summer irradiance-driven increase in energy yield.

Below, the soiling losses variability is assessed by considering only the original version of the soiling model, which does not account for the completeness of cleaning by rain. The seasonality of the soiling losses is shown in the top plot of Fig. 8 where a distinct contrast in the seasonal patterns of soiling is noticeable between southern and northern countries. Indeed, losses are predominantly seasonal in Türkiye, Portugal, Albania, Southern Italy, Spain, and Greece, because of the aforementioned long dry summer periods in which most of soiling accumulates. In these areas, indeed, most of the losses occur in August, toward the end of the dry summer. Conversely, in countries like France, Germany, Ireland, and the Benelux, losses tend to be relatively consistent (SVI <0.4) due to frequent rainfall throughout the year. The higher values recorded at Nordic latitudes, compared to central Europe, are possibly due to the low soiling losses. As the average soiling loss decreases, small seasonal variations in soiling accumulation patterns become more influential in the SVI.

The map in the bottom plot of Fig. 8 shows the interannual variability of the losses, expressed through the coefficient of variation of the annual losses calculated at each location. The larger the value, the higher the variability from one year to another. Interestingly, the locations with the highest losses are also those with the highest variability and the losses can vary by more than 100 % in some sites. The country experiencing the most variability is Portugal, with a median close to 70 %. This means that the loss varies to a significant extent relative to the mean and that monitoring is essential to assess the actual level of soiling. Countries such as Spain and Portugal are particularly exposed to Saharan dust intrusions [76], phenomena during which large portions of dust and sand are suspended and transported onto the European continent. If the suspended dust deposits on the modules, significant soiling losses can be registered even after the sky has cleared out [13]. Their stochastic nature, in terms of magnitude and frequency, is an additional possible reason for the high inter-annual variability registered in the southernmost countries. The lowest values (<10 %) are, on the other

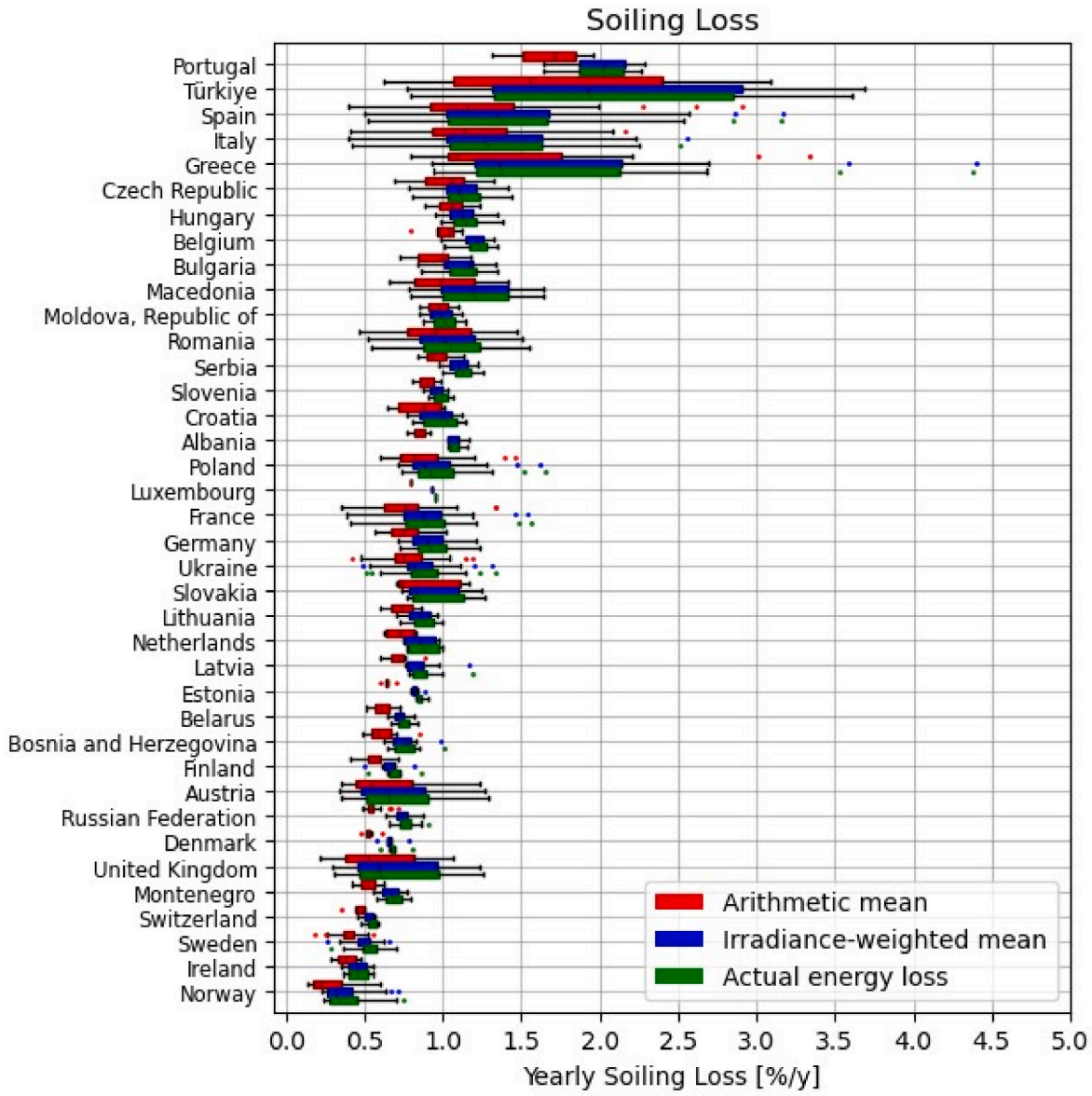

Fig. 6. Distribution of modeled soiling losses across the considered countries using the original soiling model. The distributions are created from the average soiling loss estimated for each location modeled in each country. The red bars indicate the soiling losses calculated from the arithmetic mean of the daily values ($\overline{S_L}$). The blue bars represent the irradiance-weighted mean ($\overline{S_{L\_IW}}$). The green bars indicate the energy loss due to soiling ($\overline{S_{L\_E}}$).

hand, found in countries experiencing lower losses, such as Ireland, Norway and Sweden.

3.3. Economic impact of soiling and cleanings

The plots in Fig. 9 show the economic impact of soiling across Europe if no soiling mitigation measures are taken. The presence of soiling reduces the energy yield and this leads to increases in the cost of electricity of PV. Similarly, soiling reduces the NPV, especially in those regions where both soiling losses and electricity prices are high, such as Türkiye, where any missed kWh has the maximum impact on this metric. High revenue losses are reported also in the southernmost areas of Greece, Italy, and Spain, regions of high energy yields and intense soiling.

Soiling is a reversible loss in PV. Therefore, it can be removed or prevented. As aforementioned, cleaning is the most common soiling mitigation technique. However, in order not to affect the cost-competitiveness and the profitability of PV, cleaning of the solar collectors has to lead to an adequate increase in energy yields and generate revenues higher than the cleaning costs. Ilse et al. [5] reported cleaning costs for some of the countries investigated in this work, with values ranging from a minimum of 0.07–0.09 €/m^2 in Türkiye to a maximum of 0.46–0.92 €/m^2 in the Netherlands. Assuming an electrical efficiency of 21.4 %, these correspond to cleaning costs of 0.3 €/kW to 4.3 €/kW.

The cost-effectiveness and the profitability of cleaning therefore change depending on a number of conditions: magnitude of the losses, electricity price and cleaning costs. Fig. 10 compares the actual cleaning costs reported in the assessment presented by Ilse et al. [5] with the maximum allowed costs. These maximum costs ensure that cleaning expenses do not raise the Levelized Cost of Energy (LCOE) or lower the Net Present Value (NPV). In other words, the maximum LCOE cleaning cost ensures that any increase in energy output from recovered energy offsets the cost increase due to the cleaning. Similarly, the maximum NPV cleaning cost is equal to the additional revenues one could achieve from the energy recovered through cleaning (and, therefore, does not reduce the NPV).

The results in the top plot of Fig. 10 show that, for the results derived

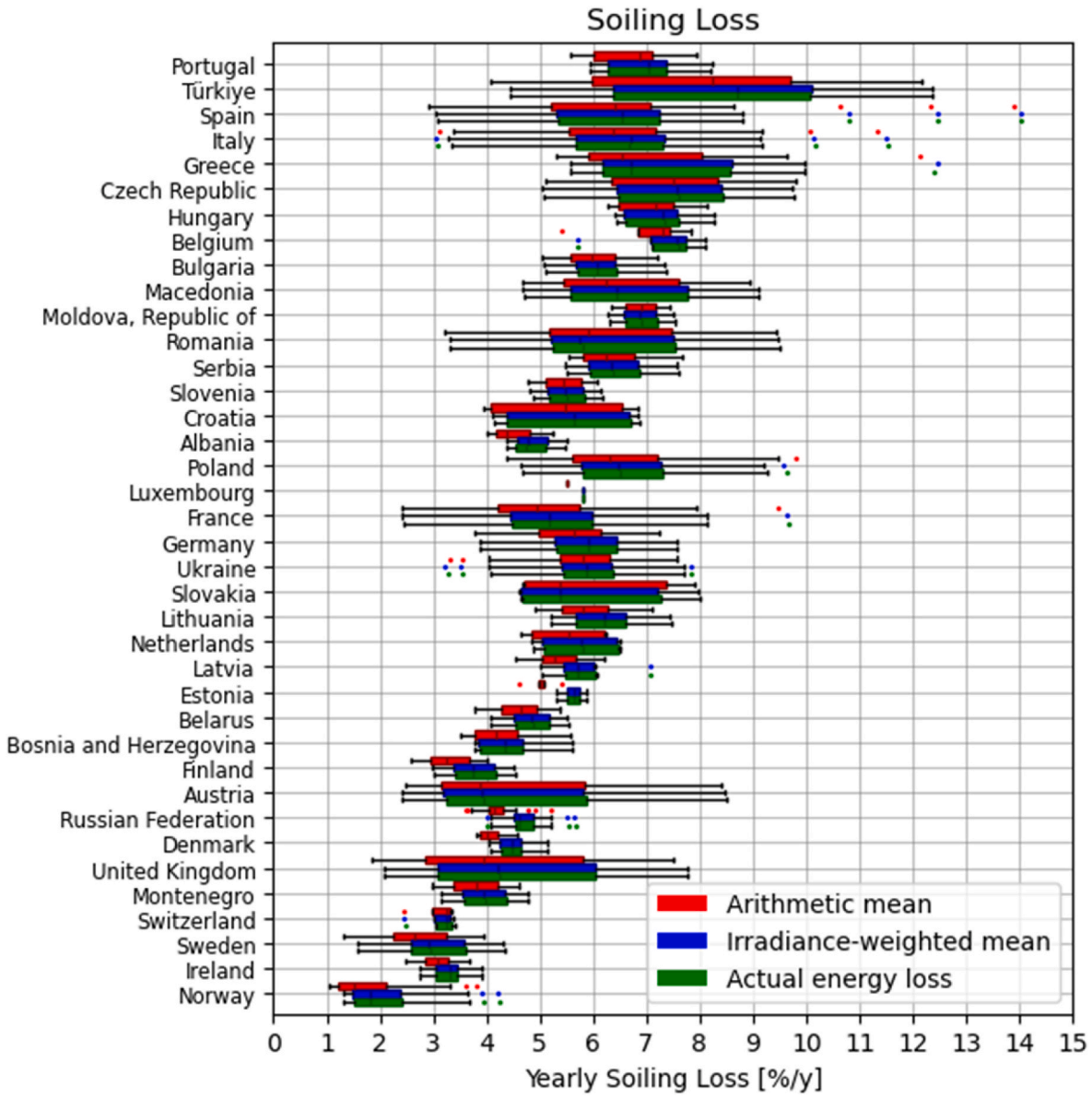

Fig. 7. Distribution of modeled soiling losses across the considered countries using the modified soiling model. The distributions are created from the average soiling loss estimated for each location modeled in each country. The red bars indicate the soiling losses calculated from the arithmetic mean of the daily values ($\overline{S_L}$). The blue bars represent the irradiance-weighted mean ($\overline{S_{L\_IW}}$). The green bars indicate the energy loss due to soiling ($\overline{S_{L\_E}}$).

from the original model, cleaning, under the assumed conditions and in the seven countries for which cleaning costs are available, is cost-effective in Türkiye and most parts of Italy and Spain. This is due to the high energy yields and the high soiling losses experienced in these areas. Furthermore, locations with high soiling seasonality tend to benefit more from cleaning, because the losses reach higher values and therefore cleanings allow for recovering a larger portion of energy yield. In Türkiye, the low cleaning costs and the high electricity prices favor the soiling mitigation activities. Despite the relatively low soiling, cleaning can be also cost-effective in the United Kingdom, because of the higher electricity prices and the lower cleaning costs compared to other non-Mediterranean countries. For the other countries, the actual cleaning costs are above those limited by LCOE and NPV. This reflects the impacts of both the soiling model's assumption of perfect cleaning by rain and the frequent rainfall in those countries.

On the other hand, the bottom plot of Fig. 10 shows the results if the modified version of the model with a cleaning completeness by rain of 10 % is applied. In this case, the results show that cleaning is cost-effective in most locations of the seven evaluated countries.

Even if cleaning is the most common mitigation technique, additional solutions can be put in place to reduce the accumulation of soiling. These include, for example, anti-soiling coatings, thin layers of material deposited on the PV module surface to reduce the soiling deposition rate and favor its natural removal [5]. Differently from cleaning, anti-soiling coatings are preventive solutions impacting the capital expenditure of a PV system. Future works should evaluate the cost-effectiveness of these solutions and provide a more comprehensive overview of the soiling mitigation potentials and challenges.

3.4. Impact of the effectiveness of rain in cleaning soiling

Table 1 compares the results between the original version of the model and the modified version that considers that rain events above the CT only remove 10 % of the accumulated soiling.

The comparison between the original and modified versions of the model reveals significant differences in the simulations. The original

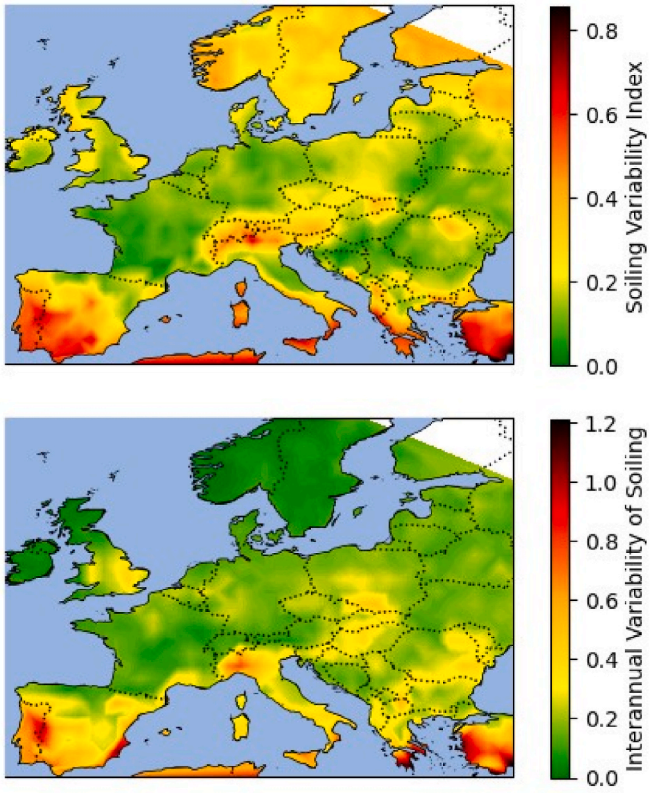

Fig. 8. Soiling Variability Index (top plot) and coefficient of variation (bottom plot), proxy of the interannual variability of soiling.

model assumes total completeness of cleaning by rain. In contrast, the modified version considers a partial effectiveness of rain, with only 10 % of the accumulated soiling being removed. This results in much higher values of soiling losses. On average, the modified model returns results that are approximately five and three times greater than those of the original version for average and peak values, respectively. This suggests that the original model may fail to account for the persistence of soiling even after significant rainfalls in some occasions or sites. On the other hand, the modified model, which assumes rain plays a minor role in soiling removal, can give a more realistic idea of how soiling can build up over time even in locations with consistent precipitations, but where soiling types have strong adhesion properties. In most of the PV installations, the completeness of cleaning by rain likely falls somewhere between the two extremes analyzed in this work, depending on local environmental conditions and the specific nature of soiling.

The profitability of manual cleanings is also largely affected by the rain's cleaning effectivity. While assuming a perfect cleaning effectivity can result in manual cleanings not being profitable in regions with low electricity prices and high cleaning costs, the opposite extreme (only 10 % cleaning effectivity) leads to manual cleaning being cost-effective in most locations.

4. Conclusions

This work presents a first continental techno-economic assessment of the soiling losses across Europe. A novel and extensive set of soiling measurements is used to calibrate the model used for soiling estimation, returning average annual energy losses up to 3.5 % or up to 14.0 % if a 10 % cleaning effectivity of rain is considered in some Mediterranean countries. This low cleaning effectivity was derived from an exemplary site in Switzerland and may represent the difficulty in cleaning some soiling types, such as brake dust. Notably, the analysis shows that calculating the impact of soiling using an arithmetic average of the daily values leads to significant underestimation of the losses. More reliable results are obtained, on the other hand, if the losses are calculated using

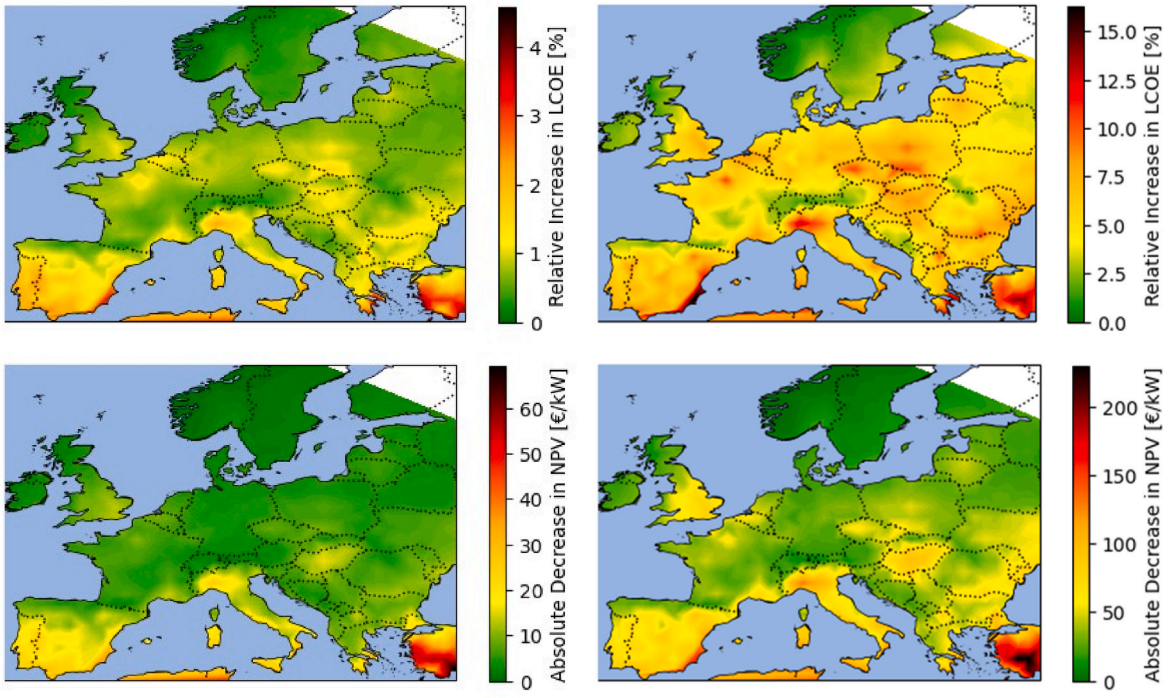

Fig. 9. Increase in LCOE (top row) and loss in revenues (bottom row) due to soiling if no soiling mitigation measures are taken. The plots in the left column correspond to the original version of the soiling model that assumes perfect cleaning by rain, while the plots in the right column represent the modified version of the soiling model assuming only partial cleaning.

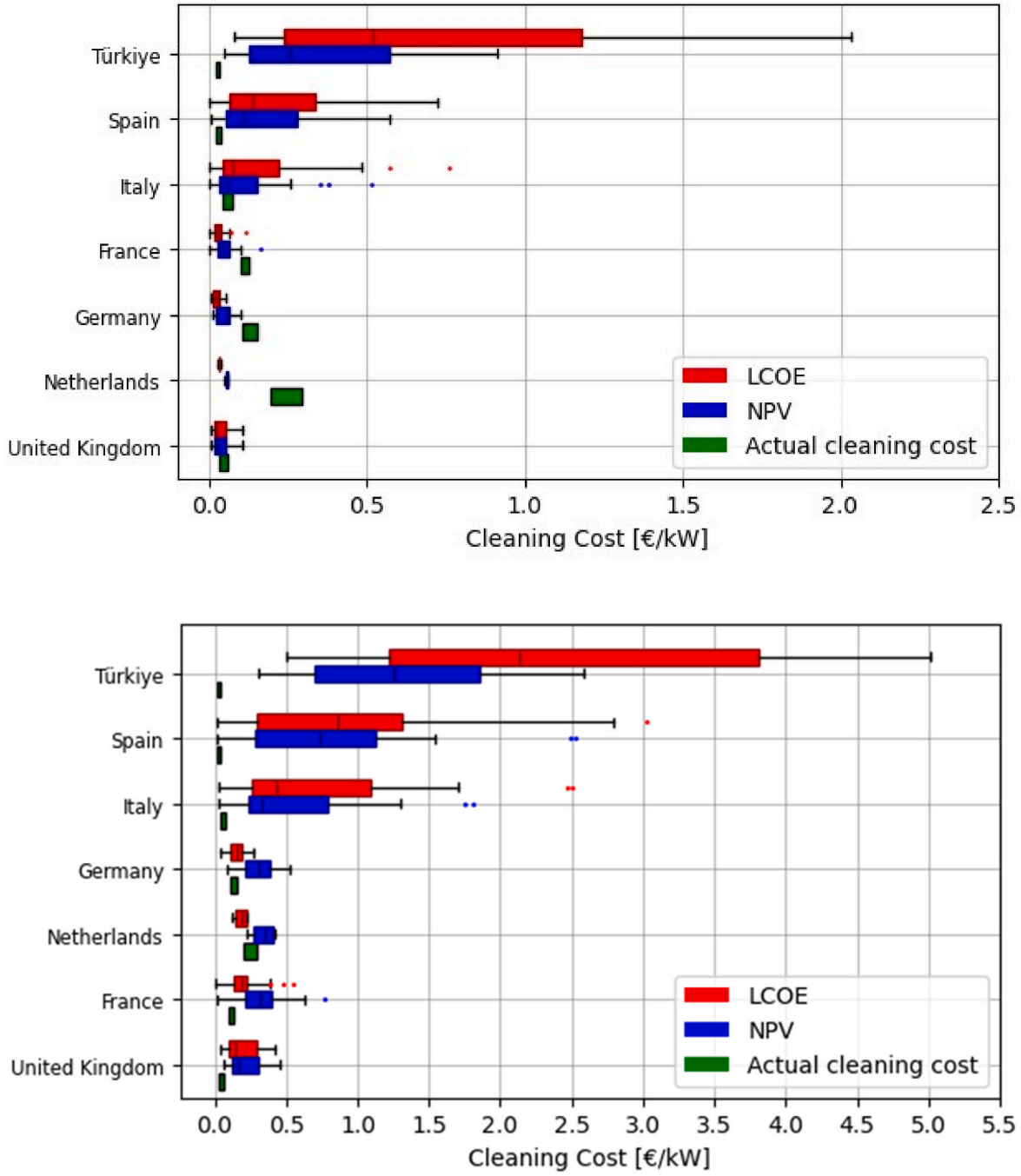

Fig. 10. Comparison of actual cleaning cost (taken from Ref. [3]) with the maximum allowed cleaning costs not to increase the LCOE or the NPV. Only countries whose cleaning costs were available in Ref. [5] are shown. Top plot: original version of the soiling model. Bottom plot: modified version of the soiling model assuming only partial cleaning by rain.

an irradiance-weighted mean because, frequently, the highest soiling losses are registered during the seasons with the greatest solar irradiation.

This work also evaluates the temporal variability of soiling, analyzing seasonality and interannual fluctuations. The regions with the highest losses are typically also those with the highest seasonality, because of the long and arid summers with usually only a few precipitation events, which can contribute in some cases to the natural cleaning of the solar collectors. This study introduces a modification of the soiling model that allows to account for the completeness of cleaning by rain. This novelty in the model can help better model those sites where there are important and/or long-term soiling losses despite the frequent precipitations.

In addition, the evaluation of the interannual variability of soiling presented in this study shows that the zones with the highest losses are also those with the greatest inter-annual variability (Türkiye and some southern regions within the Mediterranean countries of Greece, Italy, and Spain). An analysis of cleaning cost-effectiveness shows the significant profits achievable through soiling mitigation in several European countries for the assumed cleaning costs.

Future investigation should expand the present analysis by further improving the soiling estimation process using real-time data and short-term weather forecasts. Particular care should be given to understanding the mechanisms of natural cleanings, and to including additional

Table 1
Comparison between the original (perfect cleaning associated to rain events with an intensity higher than the CT) and the modified soiling model (rain events with an intensity higher than the CT only remove 10 % of the accumulated mass).

Indicator		Original soiling model (Perfect cleaning)	Modified soiling model (10 % cleaning)
Soiling magnitude In Europe	Average annual soiling loss	0.9 ± 0.4 %	5.3 ± 2.0 %
	Peak soiling loss	4.3 % (Greece)	14.0 % (Spain)
	Minimum soiling loss	0.2 % (Norway)	1.2 % (Norway)
Economic metrics	Average increase in LCOE	1.0 ± 0.5 %	5.8 ± 2.2 %
	Peak increase in LCOE	4.6 % (Türkiye)	16.3 % (Spain)
	Average reduction of NPV	9.1 ± 8.5 €/kW	45.0 ± 31.3 €/kW
	Peak reduction of NPV	69.3 €/kW (Türkiye)	230.4 €/kW (Türkiye)

parameters in the soiling deposition and removal modeling. These results would allow improving and updating the presented maps for a better estimation of the energy and economic impact of soiling and cleanings. The results and conclusions of this study will be updated in the future, as the presented findings are expected to promote the deployment of soiling monitors in additional sites. This will enable further refinement and validation of the methodology used.

CRediT authorship contribution statement

Álvaro Fernández Solas: Writing – original draft, Validation, Methodology, Investigation, Formal analysis, Data curation, Conceptualization. **Nicholas Riedel-Lyngskær:** Writing – review & editing, Resources. **Natalie Hanrieder:** Writing – review & editing, Resources. **Fernanda Norde Santos:** Writing – review & editing, Data curation. **Stefan Wilbert:** Writing – review & editing, Resources, Methodology. **Heine Nygard Riise:** Writing – review & editing, Data curation. **Jesús Polo:** Writing – review & editing, Data curation. **Eduardo F. Fernández:** Writing – review & editing. **Florencia Almonacid:** Writing – review & editing. **Diego L. Talavera:** Writing – review & editing, Validation, Methodology, Data curation. **Leonardo Micheli:** Writing – original draft, Visualization, Validation, Software, Project administration, Methodology, Investigation, Formal analysis, Data curation, Conceptualization.

Data availability

Data will be made available on request.

Declaration of generative AI and AI-assisted technologies in the writing process

During the preparation of this work some authors used ChatGPT by OpenAI in order to improve spelling, grammar, clarity, and general editing. After using this tool, the authors reviewed and edited the content as needed and take full responsibility for the content of the publication.

Declaration of competing interest

The authors declare that they have no known competing financial interests or personal relationships that could have appeared to influence the work reported in this paper.

Acknowledgments

L. Micheli's work was supported by Sole4PV, a project funded by the Italian Ministry of University and Research under the 2019 «Rita Levi Montalcini » Program for Young Researchers. H. Nygard Riise gratefully acknowledges support from the Research Council of Norway grant no. 320750. The authors would like to thank the PVCastSOIL Project (ENE2017-469 83790-C3-1, 2 and 3), which is funded by the Ministerio de Economía y Competitividad (MINECO), and co-financed by the European Regional Development Fund. The authors wish to thank Elena Ruiz Donoso (German Aerospace Center (DLR), Institute of Solar Research) for her support in reviewing the methodology and results.

Appendix A. Supplementary data

Supplementary data to this article can be found online at https://doi.org/10.1016/j.renene.2024.122086.

References

[1] European Commission, REPowerEU, A plan to rapidly reduce dependence on Russian fossil fuels and fast forward the green transition. https://ec.europa.eu/commission/presscorner/detail/en/ip_22_3131, 2022. (Accessed 20 February 2024).
[2] SolarPower Europe, EU Market Outlook for Solar Power 2023-2027, 2023.
[3] T. Sarver, A. Al-Qaraghuli, L.L. Kazmerski, A comprehensive review of the impact of dust on the use of solar energy: history, investigations, results, literature, and mitigation approaches, Renew. Sustain. Energy Rev. 22 (2013) 698–733, https://doi.org/10.1016/j.rser.2012.12.065.
[4] K.K. Ilse, B.W. Figgis, V. Naumann, C. Hagendorf, J. Bagdahn, Fundamentals of soiling processes on photovoltaic modules, Renew. Sustain. Energy Rev. 98 (2018) 239–254, https://doi.org/10.1016/j.rser.2018.09.015.
[5] K. Ilse, L. Micheli, B.W. Figgis, K. Lange, D. Daßler, H. Hanifi, F. Wolfertstetter, V. Naumann, C. Hagendorf, R. Gottschalg, J. Bagdahn, Techno-economic assessment of soiling losses and mitigation strategies for solar power generation, Joule 3 (2019) 2303–2321, https://doi.org/10.1016/j.joule.2019.08.019.
[6] M. Abraim, M. Salihi, O. El, N. Hanrieder, H. Ghennioui, A. Ghennioui, M. El, A. Azouzoute, Techno-economic assessment of soiling losses in CSP and PV solar power plants : a case study for the semi-arid climate of Morocco, Energy Convers. Manag. 270 (2023) 116285, https://doi.org/10.1016/j.enconman.2022.116285.
[7] B. Laarabi, Y. El Baqqal, N. Rajasekar, A. Barhdadi, Updated review on soiling of solar photovoltaic systems Morocco and India contributions, J. Clean. Prod. 311 (2021) 127608, https://doi.org/10.1016/j.jclepro.2021.127608.
[8] M.Z. Khan, R. Gottschalg, A.A. Alowais, M. Mirza, E. Grunwald, K. Ilse, Soiling mitigation potential of glass coatings and tracker routines in the desert climate of Saudi Arabia, 45–55, https://doi.org/10.1002/pip.3736, 2024.
[9] H.N. Riise, M. Øgaard, T.U. Naerland, Soiling and snow impact on a Pv plant at a farm in Norway, in: 38th Eur. Photovolt. Sol. Energy Conf., Exhib., 2021, pp. 1241–1244.
[10] R. Appels, B. Lefevre, B. Herteleer, H. Goverde, A. Beerten, R. Paesen, K. De Medts, J. Driesen, J. Poortmans, Effect of soiling on photovoltaic modules, Sol. Energy 96 (2013) 283–291, https://doi.org/10.1016/j.solener.2013.07.017.
[11] BBC, Saharan Dust Cloud Sweeps over UK Covering Cars in an Orange Powder, BBC, 2023. https://www.bbc.co.uk/newsround/66734529. (Accessed 11 September 2023).
[12] S. Garofalide, C. Postolachi, A. Cocean, G. Cocean, I. Motrescu, I. Cocean, B. S. Munteanu, M. Prelipceanu, S. Gurlui, L. Leontie, Saharan dust storm aerosol characterization of the event (9 to 13 may 2020) over European AERONET sites, Atmosphere 13 (2022), https://doi.org/10.3390/atmos13030493.
[13] R. Conceição, H.G. Silva, J. Mirão, M. Gostein, L. Fialho, L. Narvarte, M. Collares-Pereira, Saharan dust transport to Europe and its impact on photovoltaic performance: a case study of soiling in Portugal, Sol. Energy 160 (2018) 94–102, https://doi.org/10.1016/j.solener.2017.11.059.
[14] M. Korevaar, J. Mes, P. Nepal, G. Snijders, M.X. van, Novel soiling detection system for solar panels, in: 33rd Eur. Photovolt. Sol. Energy Conf., Exhib., 2017, https://doi.org/10.4229/EUPVSEC20172017-6BV.2.11.
[15] M. Muller, L. Micheli, A.F. Solas, M. Gostein, J. Robinson, K. Morely, M. Dooraghi, Y.A. Alghamdi, Z.A. Almutairi, F. Almonacid, E.F. Fernandez, An in-depth field validation of "DUSST": a novel low-maintenance soiling measurement device, Prog. Photovoltaics Res. Appl. 29 (2021) 953–967, https://doi.org/10.1002/pip.3415.
[16] B. Aïssa, G. Scabbia, B.W. Figgis, J. Garcia Lopez, V. Bermudez Benito, PV-soiling field-assessment of Mars™ optical sensor operating in the harsh desert environment of the state of Qatar, Sol. Energy 239 (2022) 139–146, https://doi.org/10.1016/j.solener.2022.04.064.
[17] L. Campos, S. Wilbert, J. Meyer, J. La Casa, E. Borg, F. Wolfertstetter, L. F. Zarzalejo, A. Fernández-garcía, F.N. Santos, Autonomous measurement system for photovoltaic and radiometer soiling losses, 1336–1349, https://doi.org/10.1002/pip.3650, 2023.

[18] M. Yang, J. Ji, S. Member, B. Guo, Soiling quantification using an image-based method : effects of imaging conditions, IEEE J. Photovoltaics (2020) 1–8, https://doi.org/10.1109/JPHOTOV.2020.3018257.
[19] M. Coello, L. Boyle, Simple model for predicting time series soiling of photovoltaic panels, IEEE J. Photovoltaics 9 (2019) 1382–1387, https://doi.org/10.1109/JPHOTOV.2019.2919628.
[20] S. You, Y.J. Lim, Y. Dai, C.H. Wang, On the temporal modelling of solar photovoltaic soiling: energy and economic impacts in seven cities, Appl. Energy 228 (2018) 1136–1146, https://doi.org/10.1016/j.apenergy.2018.07.020.
[21] G. Eder, G. Peharz, R. Trattnig, P. Bonomo, E. Saretta, F. Frontini, C.S. Polo Lopez, H. Rose Wilson, J. Eisenlohr, N. Martín Chivelet, S. Karlsson, N. Jakica, A. Zanelli, COLOURED BIPV Market, vol. 15, research and development IEA PVPS Task, 2019, p. 57. Report IEA-PVPS T15-07: 2019, http://iea-pvps.org/index.php?id=task15.
[22] J. Polo, N. Martín-Chivelet, C. Sanz-Saiz, J. Alonso-Montesinos, G. López, M. Alonso-Abella, F.J. Batlles, A. Marzo, N. Hanrieder, Modeling soiling losses for rooftop PV systems in suburban areas with nearby forest in Madrid, Renew. Energy 178 (2021) 420–428, https://doi.org/10.1016/j.renene.2021.06.085.
[23] A. Kimber, L. Mitchell, S. Nogradi, H. Wenger, The effect of soiling on large grid-connected photovoltaic systems in California and the southwest region of the United States, in: Photovolt. Energy Conversion, Conf. Rec. 2006 IEEE 4th World Conf, 2006, pp. 2391–2395.
[24] H. Jiang, L. Lu, K. Sun, Experimental investigation of the impact of airborne dust deposition on the performance of solar photovoltaic (PV) modules, Atmos. Environ. 45 (2011) 4299–4304, https://doi.org/10.1016/j.atmosenv.2011.04.084.
[25] L. Boyle, H. Flinchpaugh, M.P. Hannigan, Natural soiling of photovoltaic cover plates and the impact on transmission, Renew. Energy 77 (2015) 166–173, https://doi.org/10.1016/j.renene.2014.12.006.
[26] M.H. Bergin, C. Ghoroi, D. Dixit, J.J. Schauer, D.T. Shindell, Large reductions in solar energy production due to dust and particulate air pollution, Environ. Sci. Technol. Lett. 4 (2017) 339–344, https://doi.org/10.1021/acs.estlett.7b00197.
[27] W. Javed, B. Guo, B. Figgis, Modeling of photovoltaic soiling loss asa function of environmental variables, Sol. Energy 157 (2017) 397–407, https://doi.org/10.1016/j.solener.2017.08.046.
[28] S. Toth, M. Hannigan, M. Vance, M. Deceglie, Predicting photovoltaic soiling from air quality measurements, IEEE J. Photovoltaics 10 (2020) 1142–1147, https://doi.org/10.1109/JPHOTOV.2020.2983990.
[29] S. You, Y. Jie, Y. Dai, C. Wang, On the temporal modelling of solar photovoltaic soiling : energy and economic impacts in seven cities, Appl. Energy 228 (2018) 1136–1146, https://doi.org/10.1016/j.apenergy.2018.07.020.
[30] S. Sharma, G. Raina, S. Yadav, S. Sinha, A comparative evaluation of different PV soiling estimation models using experimental investigations, Energy Sustain. Dev. 73 (2023) 280–291, https://doi.org/10.1016/j.esd.2023.02.008.
[31] J.G. Bessa, L. Micheli, J. Montes-Romero, F. Almonacid, E.F. Fernández, Estimation of photovoltaic soiling using environmental parameters: a comparative analysis of existing models, Adv. Sustain. Syst. 2100335 (2022) 2100335, https://doi.org/10.1002/adsu.202100335.
[32] V. Lara-Fanego, C.A. Gueymard, L. Micheli, Soiling model for PV applications: improved parameterizations, Conf. Rec. IEEE Photovolt. Spec. Conf. (2023) 1–3, https://doi.org/10.1109/PVSC48320.2023.10359694.
[33] J. Lopez-Lorente, J. Polo, N. Martín-Chivelet, M. Norton, A. Livera, G. Makrides, G. E. Georghiou, Characterizing soiling losses for photovoltaic systems in dry climates: a case study in Cyprus, Sol. Energy 255 (2023) 243–256, https://doi.org/10.1016/j.solener.2023.03.034.
[34] M. Redondo, C.A. Platero, A. Moset, F. Rodríguez, V. Donate, Soiling modelling in large grid-connected PV plants for cleaning optimization, Energies 16 (2023) 1–13, https://doi.org/10.3390/en16020904.
[35] B. Laarabi, O. May Tzuc, D. Dahlioui, A. Bassam, M. Flota-Bañuelos, A. Barhdadi, Artificial neural network modeling and sensitivity analysis for soiling effects on photovoltaic panels in Morocco, Superlattice. Microst. 127 (2019) 139–150, https://doi.org/10.1016/j.spmi.2017.12.037.
[36] C. Schill, A. Anderson, C. Baldus-Jeursen, L. Burnham, L. Micheli, D. Parlevliet, E. Pilat, B. Stridh, E. Urreloja, M. Basappa Ayanna, G. Cattaneo, S.-J. Ernst, A. Kottantharayil, G. Mathiak, E. Whitney, R. Neukomm, D. Petri, L. Pratt, L. Rustam, T. Schott, Soiling losses – impact on the performance of photovoltaic power plants report IEA-PVPS T13-21:2022. https://iea-pvps.org/key-topics/soiling-losses-impact-on-the-performance-of-photovoltaic-power-plants/, 2022.
[37] Copernicus Atmosphere Monitoring Service (CAMS), Atmosphere Data Store, (n.d.). https://ads.atmosphere.copernicus.eu/#!/home (accessed January 19, 2024).
[38] L. Micheli, G.P. Smestad, J.G. Bessa, M. Muller, E.F. Fernandez, F. Almonacid, Tracking soiling losses: assessment, uncertainty, and challenges in mapping, IEEE J. Photovoltaics 12 (2022) 114–118, https://doi.org/10.1109/JPHOTOV.2021.3113858.
[39] Atonometrics, RDE300i PV Module Measurement System, (n.d.). https://www.atonometrics.com/products/rde300i-pv-module-measurement-system/(accessed January 31, 2024).
[40] Kipp&Zonen, DustIQ Soiling Monitoring System, (n.d.). https://www.kippzonen.com/Product/419/DustIQ-Soiling-Monitoring-System (accessed January 31, 2024).
[41] European Commission, PVGIS user manual, (n.d.). https://joint-research-centre.ec.europa.eu/photovoltaic-geographical-information-system-pvgis/getting-started-pvgis/pvgis-user-manual_en (accessed April 19, 2024).
[42] T. Huld, R. Müller, A. Gambardella, A new solar radiation database for estimating PV performance in Europe and Africa, Sol. Energy 86 (2012) 1803–1815, https://doi.org/10.1016/j.solener.2012.03.006.
[43] A.P. Dobos, A.P. Dobos, PVWatts Version 5 Manual PVWatts Version 5 Manual, 2014.
[44] A. Skomedal, M.G. Deceglie, Combined estimation of degradation and soiling losses in photovoltaic systems, IEEE J. Photovoltaics 10 (2020) 1788–1796, https://doi.org/10.1109/jphotov.2020.3018219.
[45] L. Micheli, D. Ruth, M. Muller, Seasonal trends of soiling on photovoltaic systems, in: 2017 IEEE 44th Photovolt, Spec. Conf., IEEE, Washington, D.C., 2017, https://doi.org/10.1109/PVSC.2017.8366381.
[46] R.P.D. Walsh, D.M. Lawler, Rainfall seasonality: description, spatial patterns and change through time, Weather 36 (1981) 201–208, https://doi.org/10.1002/j.1477-8696.1981.tb05400.x.
[47] M. Muller, F. Rashed, Considering the variability of soiling in long-term PV performance forecasting, IEEE J. Photovoltaics 13 (2023) 825–829, https://doi.org/10.1109/JPHOTOV.2023.3300369.
[48] W. Javed, B. Guo, B. Figgis, L. Martin Pomares, B. Aïssa, L. Martin, B. Aïssa, Multi-year field assessment of seasonal variability of photovoltaic soiling and environmental factors in a desert environment, Sol. Energy 211 (2020) 1392–1402, https://doi.org/10.1016/j.solener.2020.10.076.
[49] F. Norde Santos, S. Wilbert, E.R. Donoso, J. El Dik, L.C. Guzmán, N. Hanrieder, A. F. García, C.A. Garçia, J. Polo, A. Forstinger, R. Affolter, R. Pitz-Paal, Cleaning of PV through rain: experimental study and modelling approaches, Sol. RRL (2024), https://doi.org/10.1002/solr.202400551.
[50] L. Micheli, D.L. Talavera, Economic feasibility of floating photovoltaic power plants: profitability and competitiveness, Renew. Energy 211 (2023) 607–616, https://doi.org/10.1016/j.renene.2023.05.011.
[51] D.L. Talavera, E. Muñoz-Cerón, J.P. Ferrer-Rodríguez, P.J. Pérez-Higueras, Assessment of cost-competitiveness and profitability of fixed and tracking photovoltaic systems: the case of five specific sites, Renew. Energy 134 (2019) 902–913, https://doi.org/10.1016/j.renene.2018.11.091.
[52] D.C. Jordan, K. Anderson, K. Perry, M. Muller, M. Deceglie, R. White, C. Deline, Photovoltaic fleet degradation insights, Prog. Photovoltaics Res. Appl. 30 (2022) 1166–1175, https://doi.org/10.1002/pip.3566.
[53] W. Short, D.J. Packey, T. Holt, A Manual for the Economic Evaluation of Energy Efficiency and Renewable Energy Technologies, National Renewable Energy Laboratory, Golden, Colorado (USA), 1995.
[54] IRENA, Renewable Power Generation Costs in 2022, 2023. Abu Dhabi.
[55] IBEX Independent Bulgarian Energy Exchange, DAM Historical Data, (n.d.). https://ibex.bg/dam-history.php (accessed November 14, 2022).
[56] CROPEX Croatian power exchange, CROPEX Croatian power exchange, (n.d.). https://www.cropex.hr/en/documents.html (accessed November 14, 2020).
[57] SEEPEX, Rules and Docs, (n.d.). http://www.seepex-spot.rs/en/rules-and-docs (accessed November 14, 2022).
[58] OKTE, Total STM results, (n.d.). https://www.okte.sk/en/(accessed November 14, 2022).
[59] Borzen, Market Data Archive, (n.d.). https://ot.borzen.si/en/Home/Market-data-archive (accessed November 14, 2022).
[60] BSP Energy Exchange, BSP Energy Exchange, (n.d.). https://www.bsp-southpool.com/home.html (accessed November 14, 2022).
[61] OMIE, Day-ahead minimum, average and maximum price, (n.d.). https://www.omie.es/en/market-results/interannual/daily-market/daily-prices?scope=interannual (accessed November 14, 2022).
[62] PwC Turkey, Investment Office of Presidency of the Republic of Turkey, Overview of the Turkish Electricity Market, (n.d.). https://www.pwc.com.tr/overview-of-the-turkish-electricity-market (accessed November 14, 2022).
[63] Market Operator, DAM results, (n.d.). https://www.oree.com.ua/index.php/control/results_mo/DAM (accessed November 14, 2022).
[64] Ofgem - the energy regulator for Great Britain, Wholesale market indicators, (n.d.). https://www.ofgem.gov.uk/energy-data-and-research/data-portal/wholesale-market-indicators (accessed November 14, 2022).
[65] OTE (Czech electricity and gas market operator), Daily Market - Spot Market Index, (n.d.). https://www.ote-cr.cz/en/about-ote/main-reading-1 (accessed November 14, 2022).
[66] EEX group, KWK Index, (n.d.). https://www.eex.com/en/market-data/power/kwk-index (accessed November 14, 2022).
[67] EnEx, Energy Markets, (n.d.). https://www.enexgroup.gr/web/guest/energy-markets (accessed November 14, 2022).
[68] IPTO Independent Power Transmission Operator, Weighted Average Market Price, (n.d.). https://www.admie.gr/en/market/reports/weighted-average-market-price (accessed November 14, 2022).
[69] HUPX, Historical data, (n.d.). https://hupx.hu/en/market-data/dam/historical-data (accessed November 14, 2022).
[70] GME (Gestore Mercati Energetici), Comparison of European exchanges, (n.d.). https://www.mercatoelettrico.org/En/Statistiche/ME/BorseEuropee.aspx (accessed November 14, 2022).
[71] TGE, TGE Services, (n.d.). https://www.tge.pl/TGE_Services (accessed November 14, 2022).
[72] opcom, Block Prices, (n.d.). https://www.opcom.ro/rapoarte/pzu/preturi_blocuri.php?lang=en (accessed November 14, 2022).
[73] N. Hanrieder, S. Wilbert, F. Wolfertstetter, J. Polo, C. Alonso, L.F. Zarzalejo, Why natural cleaning of solar collectors cannot be described using simple rain sum thresholds, Proc. - ISES Sol. World Congr. 2021 (2021) 959–969, https://doi.org/10.18086/swc.2021.37.02.
[74] P. Virtanen, R. Gommers, T.E. Oliphant, M. Haberland, T. Reddy, D. Cournapeau, E. Burovski, P. Peterson, W. Weckesser, J. Bright, S.J. van der Walt, M. Brett, J. Wilson, K.J. Millman, N. Mayorov, A.R.J. Nelson, E. Jones, R. Kern, E. Larson, C. J. Carey, İ. Polat, Y. Feng, E.W. Moore, J. VanderPlas, D. Laxalde, J. Perktold, R. Cimrman, I. Henriksen, E.A. Quintero, C.R. Harris, A.M. Archibald, A.H. Ribeiro, F. Pedregosa, P. van Mulbregt, A. Vijaykumar, A. Pietro Bardelli, A. Rothberg,

A. Hilboll, A. Kloeckner, A. Scopatz, A. Lee, A. Rokem, C.N. Woods, C. Fulton, C. Masson, C. Häggström, C. Fitzgerald, D.A. Nicholson, D.R. Hagen, D. V. Pasechnik, E. Olivetti, E. Martin, E. Wieser, F. Silva, F. Lenders, F. Wilhelm, G. Young, G.A. Price, G.L. Ingold, G.E. Allen, G.R. Lee, H. Audren, I. Probst, J. P. Dietrich, J. Silterra, J.T. Webber, J. Slavič, J. Nothman, J. Buchner, J. Kulick, J. L. Schönberger, J.V. de Miranda Cardoso, J. Reimer, J. Harrington, J.L. C. Rodríguez, J. Nunez-Iglesias, J. Kuczynski, K. Tritz, M. Thoma, M. Newville, M. Kümmerer, M. Bolingbroke, M. Tartre, M. Pak, N.J. Smith, N. Nowaczyk, N. Shebanov, O. Pavlyk, P.A. Brodtkorb, P. Lee, R.T. McGibbon, R. Feldbauer, S. Lewis, S. Tygier, S. Sievert, S. Vigna, S. Peterson, S. More, T. Pudlik, T. Oshima, T.J. Pingel, T.P. Robitaille, T. Spura, T.R. Jones, T. Cera, T. Leslie, T. Zito, T. Krauss, U. Upadhyay, Y.O. Halchenko, Y. Vázquez-Baeza, SciPy 1.0: fundamental algorithms for scientific computing in Python, Nat. Methods 17 (2020) 261–272, https://doi.org/10.1038/s41592-019-0686-2.

[75] Á.F. Solas, E.F. Fernández, L. Micheli, N. Riedel-Lyngskær, The impact of soiling in Europe: estimation and error induced by typical loss assumptions, in: 40th Eur. Photovolt. Sol. Energy Conf., Exhib., Lisbon, Portugal, 2023.

[76] UN News, UN issues global alert to combat severe sand and dust storms, UN News (2023). (Accessed 1 November 2023). https://news.un.org/feed/view/en/story/2023/07/1138627?_gl=1*1hwvow8*_ga*NTUwNjY4NTMuMTY5NDE2NTc4MA..*_ga_TK9BQL5X7Z*MTY5NDQzMjk1MS4yLjAuMTY5NDQzMjk1Ny4wLjAuMA.